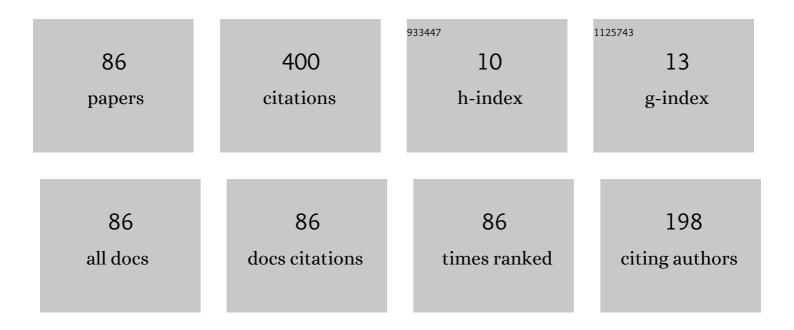


## List of Publications by Year in descending order

Source: https://exaly.com/author-pdf/4905702/publications.pdf Version: 2024-02-01



AELIM

#	Article	IF	CITATIONS
1	Dynamic motions of organic cation in organic–inorganic hybrid 1,4-butanediammonium tetrabromocuprate (II) crystal by solid-state nuclear magnetic resonance spectroscopy. Journal of Molecular Structure, 2022, 1252, 132204.	3.6	2
2	Study on structural geometry and dynamic property of [NH3(CH2)5NH3]CdCl4 crystal at phases I, II, and III. Scientific Reports, 2022, 12, 4251.	3.3	1
3	Advances in physicochemical characterization of lead-free hybrid perovskite [NH3(CH2)3NH3]CuBr4 crystals. Scientific Reports, 2022, 12, .	3.3	5
4	Structures, phase transitions, thermodynamic properties, and structural dynamics of eco-friendly hybrid perovskite NH3(CH2)3NH3CoCl4 and NH3(CH2)5NH3CoCl4 crystals. Solid State Sciences, 2022, , 106927.	3.2	2
5	Characterization on Lead-Free Hybrid Perovskite [NH3(CH2)5NH3]CuCl4: Thermodynamic Properties and Molecular Dynamics. Molecules, 2022, 27, 4546.	3.8	3
6	Thermal, ferroelastic, and structural properties near phase transitions of organic–inorganic perovskite type [NH <sub>3</sub> (CH <sub>2</sub> ) <sub>3</sub> NH <sub>3</sub> ]CdBr <sub>4</sub> crystals. RSC Advances, 2021, 11, 17622-17629.	3.6	5
7	Thermodynamic Property and Solid-State Molecular Dynamics of Cs2MnBr4·2H2O Crystal. Applied Magnetic Resonance, 2021, 52, 211-219.	1.2	1
8	Thermal property, structural characterization, and physical property of cation and anion in organic–inorganic perovskite [(CH2)3(NH3)2]CdCl4 crystal. Journal of Solid State Chemistry, 2021, 295, 121909.	2.9	6
9	Physicochemical properties and structural dynamics of organic–inorganic hybrid [NH3(CH2)3NH3]ZnX4 (X = Cl and Br) crystals. Scientific Reports, 2021, 11, 8408.	3.3	14
10	Effect of Methylene Chain Length on the Thermodynamic Properties, Ferroelastic Properties, and Molecular Dynamics of the Perovskite-type Layer Crystal [NH <sub>3</sub> (CH <sub>2</sub> ) <sub><i>n</i></sub> NH <sub>3</sub> ]MnCl <sub>4</sub> ( <i>n</i> =)	ſj ETĈŹqO O	0 rgBT /Overl
11	A prospect of cost-effective handling and transportation of graphene oxides: folding and redispersion of graphene oxide microsheets. Nanotechnology, 2021, 32, 455601.	2.6	1
12	Physicochemical properties of the cation in organic–inorganic perovskite [NH3(CH2)4(NH3)]ZnBr4 crystals investigated using 1H and 13C nuclear magnetic resonance relaxation. Journal of Solid State Chemistry, 2021, 302, 122438.	2.9	4
13	Physicochemical Property Investigations of Perovskite-Type Layer Crystals [NH <sub>3</sub> (CH <sub>2</sub> ) <sub><i>n</i></sub> NH <sub>3</sub> ]CdCl <sub>4</sub> ( <i>n</i> =) T	j ET <b>Qq1</b> 1	0.7 <b>8</b> 4314 rgB
14	Effect of methylene chain length of perovskite-type layered [NH3(CH2)nNH3]ZnCl4 (n = 2, 3, and 4) crystals on thermodynamic properties, structural geometry, and molecular dynamics. RSC Advances, 2021, 11, 37824-37829.	3.6	6
15	Effect of Proton Substitution in Li2RbH(SO4)2 Single Crystal Studied by Nuclear Magnetic Resonance Relaxation. Applied Magnetic Resonance, 2020, 51, 1-9.	1.2	Ο
16	Thermal decomposition and structural dynamics in perovskite (C2H5NH3)2CdCl4 crystals. Journal of Thermal Analysis and Calorimetry, 2020, 142, 2243-2249.	3.6	2
17	Thermal property and structural molecular dynamics of organic–inorganic hybrid perovskite 1,4-butanediammonium tetrachlorocuprate. RSC Advances, 2020, 10, 34800-34805.	3.6	6
18	Structural dynamics of CH3NH3+ and PbBr3â^' in tetragonal and cubic phases of CH3NH3PbBr3 hybrid perovskite by nuclear magnetic resonance. Scientific Reports, 2020, 10, 13140.	3.3	8

Ae Lim

#	Article	IF	CITATIONS
19	Thermal stability, cation dynamics, and ferroelastic domain walls in the α→β→γ phase transitions of perovskite (C2H5NH3)2MnCl4 crystals. Solid State Sciences, 2020, 107, 106365.	3.2	1
20	Structural characterization, thermal properties, and molecular motions near the phase transition in hybrid perovskite [(CH2)3(NH3)2]CuCl4 crystals: 1H, 13C, and 14N nuclear magnetic resonance. Scientific Reports, 2020, 10, 20853.	3.3	8
21	Dynamics of NH3(CH2)2NH3 cation in perovskite layer crystal NH3(CH2)2NH3CuCl4 by M. Solid State Communications, 2020, 312, 113862.	1.9	4
22	Determining effect of partial substitution of paramagnetic Mn2+ ions in perovskite (MA)2Zn1-Mn Cl4 mixed crystals through MAS NMR relaxation times. Solid State Sciences, 2020, 103, 106185.	3.2	0
23	Thermodynamic, Physical, and Structural Characteristics in Layered Hybrid Type (C2H5NH3)2MCl4 (M =) Tj ETQq1	1. <b>0.784</b> 3	314 rgBT /O
24	Thermodynamic Properties, Structural Characteristics, and Cation Dynamics of Perovskite-Type Layer Crystal [NH3(CH2)2NH3]ZnCl4. ACS Omega, 2020, 5, 31417-31422.	3.5	6
25	Study on Paramagnetic Interactions of (CH3NH3)2CoBr4 Hybrid Perovskites Based on Nuclear Magnetic Resonance (NMR) Relaxation Time. Molecules, 2019, 24, 2895.	3.8	9
26	Molecular dynamics of hybrid halide perovskite (CH3NH3)2CuX4 (X = Br and Cl) determined by nuclear magnetic resonance relaxation processes. Solid State Sciences, 2019, 96, 105955.	3.2	2
27	Effect of the partial substitution of Zn2+ ions in (CH3NH3)2ZnCl4 with Co2+ ions on the structure, phase transition, and molecular motion. Journal of Molecular Structure, 2019, 1195, 179-183.	3.6	1
28	Interpretation of the crystal growth, phase transition, and molecular dynamics of [N(CH3)4]2ZnBr4 crystals by replacing partially the Zn2+ ions with Co2+ ions. Journal of Molecular Structure, 2019, 1197, 471-477.	3.6	1
29	Thermotropic Liquid Crystalline Polymers with Various Alkoxy Side Groups: Thermal Properties and Molecular Dynamics. Polymers, 2019, 11, 992.	4.5	8
30	Preparation, Thermal, and Physical Properties of Perovskite-Type (C3H7NH3)2CdCl4 Crystals. Crystals, 2019, 9, 108.	2.2	2
31	Effects of paramagnetic interactions by the partial replacement of Zn2+ions with Cu2+ions in lead-free zinc-based perovskite (MA)2ZnCl4crystal by MAS NMR. AIP Advances, 2019, 9, 105115.	1.3	5
32	Thermal and structural properties, and molecular dynamics in organic–inorganic hybrid perovskite (C2H5NH3)2ZnCl4. RSC Advances, 2019, 9, 38032-38037.	3.6	3
33	Structural changes, thermodynamic properties, 1H magic angle spinning NMR, and 14N NMR of (NH4)2CuCl4·2H2O. RSC Advances, 2018, 8, 6502-6506.	3.6	2
34	Thermodynamic properties and NMR study of tetragonal tetrahalogen-metallate dihydrate crystals of Rb2[CuX4]·2H2O (X = Clâ~' and Brâ~'). Journal of Thermal Analysis and Calorimetry, 2018, 134, 1145-11	130.	0
35	Role of NH4 ions in successive phase transitions of perovskite type (NH4)2ZnX4 (X = Cl, Br) by 1H MAS NMR and 14N NMR. RSC Advances, 2018, 8, 11316-11323.	3.6	1
36	Cation dynamics by 1H and 13C MAS NMR in hybrid organic–inorganic (CH3CH2NH3)2CuCl4. RSC Advances, 2018, 8, 34110-34115.	3.6	5

#	Article	IF	CITATIONS
37	Structural geometry of the layered perovskite-type (CH3CH2CH2NH3)2CuCl4 single crystal near phase transition temperatures. AIP Advances, 2018, 8, 105324.	1.3	4
38	Ionic dynamics of the cation in organic–inorganic hybrid compound (CH <sub>3</sub> NH <sub>3</sub> ) <sub>2</sub> MCl <sub>4</sub> (M = Cu and Zn) by <sup>1</sup> H MAS NMR, <sup>13</sup> C CP MAS NMR, and <sup>14</sup> N NMR. RSC Advances, 2018, 8, 18656-18662.	3.6	14
39	Phase-transition-like phenomenon of NH4H2PO4 observed using MAS NMR and static NMR near characteristic temperature. Journal of Thermal Analysis and Calorimetry, 2017, 130, 885-889.	3.6	1
40	Tetragonal-orthorhombic-tetragonal phase transitions in organic-inorganic perovskite-type (CH 3 NH) Tj ETQq0 0	0 <sub>1</sub> gBT /O	verlock 10 Tf
41	Hysteresis effect of ammonium and water protons by 1H MAS NMR in (NH4)2CuBr4·2H2O. Journal of Molecular Structure, 2017, 1146, 324-328.	3.6	2
42	Structural changes near phase transition temperatures for the [N(C2H5)4] groups in hydrated [N(C2H5)4]2CuCl4·xH2O. Journal of Thermal Analysis and Calorimetry, 2017, 130, 879-884.	3.6	4

43	Resonance Frequency and NMR Relaxation Times in Two Inequivalent 133Cs in Cs2CuBr4 and Cs2ZnBr4 Single Crystals. Applied Magnetic Resonance, 2017, 48, 889-899.	1.2	1
44	Behavior of H <sub>2</sub> O surrounding NH <sub>4</sub> <sup>+</sup> and Al <sup>3+</sup> in NH <sub>4</sub> Al(SO <sub>4</sub> ) <sub>2</sub> ·12H <sub>2</sub> O by <sup>1</sup> H MAS NMR, <sup>14</sup> N NMR, and <sup>27</sup> Al NMR. RSC Advances, 2017, 7, 55276-55281.	3.6	6
45	Structural Phase Transition of Perovskite-Type N(CH3)4CdBr3 Studied by MAS NMR and Static NMR. Applied Magnetic Resonance, 2017, 48, 297-305.	1.2	0
46	Structural phase transitions and ferroelastic properties of perovskite-type layered (CH3NH3)2CdCl4. Journal of Applied Physics, 2017, 121, 215501.	2.5	6
47	Study of the ferroelastic phase transition in the tetraethylammonium compound [N(C2H5)4]2ZnBr4 by magic-angle spinning and static NMR. AIP Advances, 2016, 6, .	1.3	8
48	Study of Two Inequivalent Hydrogen Bonds in KHSO4 Single Crystals Using Nuclear Magnetic Resonance. Applied Magnetic Resonance, 2016, 47, 1171-1177.	1.2	0
49	Study of chemically inequivalent N(CH3)4 ions in [N(CH3)4]2ZnBr4 near the phase transition temperature using 1H MAS NMR, 13C CP/MAS NMR, and 14N NMR. Solid State Sciences, 2016, 52, 37-41.	3.2	7
50	Structural and thermodynamic properties of Tutton salt K2Zn(SO4)2·6H2O. Journal of Thermal Analysis and Calorimetry, 2016, 123, 371-376.	3.6	13
51	1H and 2H Magic Angle Spinning Nuclear Magnetic Resonance Study of Phase Transition in KH3(SeO3)2 and Deuterated KD3(SeO3)2. Applied Magnetic Resonance, 2015, 46, 1293-1300.	1.2	1
52	Nuclear quadrupole coupling parameters and structural nature of the nonlinear optical material Li 2 B 4 O 7 by NMR. Solid State Nuclear Magnetic Resonance, 2015, 66-67, 40-44.	2.3	2
53	Crystal growth and thermal properties of the Tutton salt Cs2Fe(SO4)2·6H2O single crystal. Journal of	3.6	3

<sup>54</sup>Structural characteristics for phase transitions of [N(CH3)4]2CuCl4 by 13C CP/MAS NMR and 14N NMR.<br/>Solid State Nuclear Magnetic Resonance, 2015, 70, 43-47.2.32

Ae Lim

#	Article	IF	CITATIONS
55	Thermodynamic properties and phase transitions of Tutton salt (NH4)2Fe(SO4)2·6H2O from MAS NMR and single-crystal NMR. Journal of Thermal Analysis and Calorimetry, 2014, 116, 779-783.	3.6	5
56	Structural Nature of 7Li and 11B Sites by Static NMR and MAS NMR in Nonlinear Optical Material LiCsB6O10. Applied Magnetic Resonance, 2014, 45, 169-178.	1.2	0
57	High-Temperature Phase Transition in N(CH3)4CdCl3 Studied Using Static NMR and MAS NMR. Applied Magnetic Resonance, 2014, 45, 9-17.	1.2	1
58	Thermodynamic properties and molecular dynamics of (NH4)2Zn(SO4)2·6H2O studied by single-crystal NMR and MAS NMR. Journal of Thermal Analysis and Calorimetry, 2013, 114, 699-703.	3.6	1
59	Nuclear magnetic resonance study of superprotonic conductor Rb4LiH3(SO4)4 single crystals. Solid State Nuclear Magnetic Resonance, 2013, 54, 41-46.	2.3	0
60	Ordering of the O(2)…D… O(2) bonds near the phase transition in KD3(SeO3)2 single crystals by D nuclear magnetic resonance. Open Physics, 2013, 11, .	1.7	0
61	Structural properties of mixed (NH4)2â^'xRbxZnCl4 (x=0, 1, and 2) crystals studied by 1H and 87Rb nuclear magnetic resonance. Journal of Solid State Chemistry, 2013, 200, 227-231.	2.9	2
62	2H and 133Cs nuclear magnetic resonance study of Cs3D(SO4)2 single crystals in laboratory and rotating frames. Journal of Molecular Structure, 2013, 1031, 234-238.	3.6	6
63	Thermodynamic properties and phase transitions of Tutton salt (NH4)2Co(SO4)2·6H2O crystals. Journal of Thermal Analysis and Calorimetry, 2012, 109, 1619-1623.	3.6	17
64	1H and 133Cs nuclear magnetic resonance study of the NH4 and Cs occupation rates of mixed (NH4)2â^'xCsxZnCl4 (x=0, 1, and 2) crystals. Chemical Physics, 2012, 400, 39-43.	1.9	3
65	A nuclear magnetic resonance study of the structural properties and molecular motions of Li2KH(SO4)2 and LiKSO4 single crystals. Physica B: Condensed Matter, 2012, 407, 833-837.	2.7	1
66	Nuclear Magnetic Resonance Relaxation Study of the Phase Transitions of Rb2CuCl4·2H2O and Cs2MnCl4·2H2O Single Crystals. Applied Magnetic Resonance, 2012, 42, 89-100.	1.2	3
67	Study of the molecular dynamics and phase transitions of (, Rb, and Cs) single crystals. Solid State Communications, 2011, 151, 1631-1634.	1.9	7
68	1H, 7Li, and 23Na NMR study of the relaxation processes and molecular motions of Li2NaH(SO4)2·H2O single crystals. Materials Chemistry and Physics, 2011, 131, 471-476.	4.0	1
69	Study on the structural properties and relaxation mechanisms in LiRb1â~'x(NH4)xSO4 (x=0, 0.5, and 1) mixed crystals by 1H, 7Li, and 87Rb nuclear magnetic resonance. Solid State Nuclear Magnetic Resonance, 2011, 39, 14-20.	2.3	1
70	Nuclear magnetic resonance study of the phase transitions and local environments of α-alum NH4Al(SO4)2·12H2O single crystals. Chemical Physics, 2010, 371, 91-95.	1.9	8
71	NMR study of the relaxation mechanisms in single crystals of the nonlinear optical material bismuth triborate. Physica Status Solidi (B): Basic Research, 2010, 247, 2290-2294.	1.5	5
72	H 1 and L7i nuclear magnetic resonance study of the superionic crystals K4LiH3(SO4)4 and (NH4)4LiH3(SO4)4. Journal of Applied Physics, 2010, 107, .	2.5	10

Ae Lim

#	Article	IF	CITATIONS
73	Study on the phase transitions by nuclear magnetic resonance of α-type RbAl(SO4)2·12H2O and β-type CsAl(SO4)2·12H2O single crystals. Solid State Nuclear Magnetic Resonance, 2009, 36, 45-51.	2.3	10
74	A nuclear magnetic resonance study of the phase transitions and electric quadrupole Raman processes of M5H3(SO4)4·H2O (M=Na, K, Rb, and Cs) single crystals. Solid State Nuclear Magnetic Resonance, 2009, 36, 52-59.	2.3	10
75	1H and 87Rb nuclear magnetic resonance study of the order–disorder phase transition of RbHSeO4 single crystals. Solid State Nuclear Magnetic Resonance, 2008, 34, 162-166.	2.3	1
76	Dynamics of NaHSeO3 and NaHSeO4 single crystals by observation of 1H and 23Na spin-lattice relaxation. Solid State Nuclear Magnetic Resonance, 2007, 31, 124-130.	2.3	4
77	Superionic phase transitions and nuclear spin phonon relaxation by Raman processes in Me3H(SeO4)2(Me = Na, K, and Rb) single crystals by1H and Me NMR. Journal of Physics Condensed Matter, 2007, 19, 116216.	1.8	11
78	Transferred hyperfine field of Rb2CoCl4 single crystals in the ferroelectric–incommensurate–normal phase by 87Rb NMR. Solid State Communications, 2006, 138, 22-25.	1.9	5
79	M and1H NMR, ionic motions and phase transitions in proton conducting MHSO4 (M = K, Rb, Cs, and) Tj ETQq1	1 0.78431 1.5	.4 rgBT /Overl
80	7Li and 133Cs spin–lattice relaxation in a nonlinear optical crystal CsLiB6O10. Solid State Communications, 2002, 122, 207-211.	1.9	2
81	Nuclear magnetic resonance study of 7Li and 133Cs in a nonlinear optical CsLiB6O10 single crystal. Solid State Communications, 2002, 123, 505-510.	1.9	5
82	Raman process studied by 87Rb spin-lattice relaxation in a Rb2ZnCl4 single crystal at low temperature. Solid State Communications, 2001, 118, 453-457.	1.9	14
83	Tetrahedral structure in LiKSO 4 crystals studied by 7 Li and 39 K NMR. Journal of Physics and Chemistry of Solids, 2001, 62, 881-885.	4.0	5
84	Molecular Motion Studied by Proton Magnetic Resonance in a [N(CH3)4]2ZnCl4 Single Crystal. Physica Status Solidi (B): Basic Research, 2000, 219, 389-394.	1.5	13
85	The T1ï•13C spin-lattice relaxation time of interpenetrating networks by solid state NMR. Solid State Communications, 1999, 109, 465-470.	1.9	14
86	7Li Spin-Lattice Relaxation Time in a LiNH4SO4 Single Crystal. Physica Status Solidi (B): Basic Research, 1999, 214, 375-379.	1.5	9